Journal of the American College of Cardiology Vol. 47, No. 6, 2006

Published by Elsevier Inc.
ISSN 0735-1097/06/$32.00
doi:10.1016/j.jacc.2005.12.023

Sodium-Calcium Exchange Initiated by the Ca^{2+} Transient

An Arrhythmia Trigger Within Pulmonary Veins

Eugene Patterson, PHD,* Ralph Lazzara, MD, FACC,* Bela Szabo, MD, PHD,* Hong Liu, PHD,† David Tang, MS,† Yu-Hua Li, PHD,† Benjamin J. Scherlag, PHD, FACC,* Sunny S. Po, PHD, MD*

Oklahoma City and Norman, Oklahoma

OBJECTIVES The hypothesis that an increased or prolonged Ca^{2+} transient during an abbreviated action potential can give rise to early afterdepolarizations (EADs) and triggered arrhythmia by enhanced forward sodium-calcium (Na-Ca) exchange was examined.

BACKGROUND Because pulmonary veins have the shortest action potential of any cardiac tissue, we examined this hypothesis in canine pulmonary vein sleeves during interventions further shortening the action potential and increasing the calcium transient.

METHODS Extracellular bipolar electrode, intracellular microelectrode, and isometric force (a surrogate marker for the Ca^{2+} transient) recordings were obtained from superfused canine pulmonary veins.

RESULTS An elevation and prolongation of the terminal phase of repolarization (EADs) were observed during interventions increasing contractile force; isoproterenol or norepinephrine (3.2×10^{-11} to 3.2×10^{-7}M), hypothermia, and pacing (post-extrasystolic potentiation, post-pacing pause). The EAD formation was prevented by ryanodine (10 μM) or reversed by transiently increasing $[Ca^{2+}]_o$ from 1.35 to 5 mM (inhibition of forward Na-Ca exchange). Pacing-induced EADs were enhanced by re-introduction of normal Tyrode solution (Na^+ = 130 mM) after substitution of 30 mM NaCl with 30 mM LiCl (stimulation of forward Na-Ca exchange). With norepinephrine or isoproterenol (3.2×10^{-8}M) + acetylcholine (10^{-7}M) (to enhance the Ca^{2+} transient and further shorten the abbreviated action potential, respectively), tachycardia-pause initiated arrhythmia (1,132 ± 153 beats/min) lasting >1 s was observed. Rapid firing was prevented by either suppression of the Ca^{2+} transient (ryanodine) or transiently increasing $[Ca^{2+}]_o$.

CONCLUSIONS The data show EAD formation in superfused canine pulmonary veins, enhanced by an increased Ca^{2+} transient and increased Na-Ca exchange current. With subsequent shortening of the action potential with acetylcholine, tachycardia-pause triggers rapid firing within the PV sleeve. (J Am Coll Cardiol 2006;47:1196–206) © 2006 by the American College of Cardiology Foundation

Rapid focal excitation originating within left atrial myocardial extensions into the pulmonary veins (PVs) is the initiator for atrial fibrillation (AF) in the great majority of patients presenting for electrophysiological study (1). Focal firing >500/min has been reported (1,2). Coupling intervals of PV-derived premature beats are short, and refractory periods as brief as 60 ms have been reported (3).

The ionic mechanisms for focal firing have not been clarified. Studies of isolated PV myocytes and multicellular PV preparations disclose action potentials of brief duration (4–8) and excitation during repolarization described as early afterdepolarizations (EADs) (5–7). These observations conform with clinical findings of brief refractory periods and short coupling intervals for excitation originating within PVs (3). These EADs contrast with previously studied EADs associated with prolonged repolarization (9–11). Although local re-excitation may also result from circus movement (re-entry) (12–15) or phase II re-entry (16), these mechanisms cannot be operative in isolated myocytes. The brief action potential duration (APD) and the short coupling interval for spontaneous excitation during repolarization led us to examine the hypothesis that triggered excitation could result from forward sodium-calcium (Na-Ca) exchange (NCX) and an inward current (I_{NCX}) activated by the elevated $[Ca^{2+}]_i$, a circumstance favored by accelerated repolarization and enhancement/delay of the Ca^{2+} transient. The brief APDs of PV myocytes provide an intrinsic vulnerability to "Ca^{2+} transient triggering" under conditions exaggerating temporal asynchrony between repolarization and the Ca^{2+} transient.

We manipulated by experimental interventions the duration of repolarization, the amplitude and duration of the Ca^{2+} transient, and NCX in superfused canine PV tissue preparations. Membrane voltage, triggering, and contractile force (an index of $[Ca^{2+}]_i$ during the Ca^{2+} transient) were measured to establish an association between an enhanced Ca^{2+} transient, increased inward I_{NCX} and EAD formation, and arrhythmia formation.

From the *University of Oklahoma Health Sciences Center and the DVA Medical Center, Oklahoma City, Oklahoma; and the †University of Oklahoma, College of Engineering, School of Electrical and Computer Engineering, Norman, Oklahoma. The studies were supported by a research grant from the American Heart Association, Heartland Affiliate.

Manuscript received May 31, 2005; revised manuscript received August 18, 2005, accepted September 8, 2005.

Abbreviations and Acronyms

AF = atrial fibrillation
APD = action potential duration
EAD = early afterdepolarization
I_{NCX} = inward current sodium-calcium exchange
Na-Ca = sodium-calcium
NCX = sodium-calcium exchange
PV = pulmonary vein

METHODS

Male dogs (n = 50) were anesthetized with intravenous sodium pentobarbital. The heart was excised and placed into Tyrode solution containing (mM): NaCl, 130; KCl, 4.0; $MgCl_2$, 1.0; $NaHCO_3$, 20; NaH_2PO_4, 1.0; glucose, 5.5; and $CaCl_2$, 1.35, bubbled with 95% oxygen: 5% CO_2 (pH, 7.40 to 7.45). Preparations containing the PV antrum, the visible PV myocardial sleeve, and 3 to 5 mm of the PV distal to the visible sleeve were excised and dissected free of residual adipose and visceral tissues. The preparations were cut lengthwise and pinned for superfusion of the endocardial surface (20 ml/min).

Electrical recordings. Up to three bipolar electrograms (0.10 mm diameter Teflon-coated silver wires, 1 mm apart) and an intracellular glass microelectrode (3 M KCl, 10 to 30 MΩ) were recorded on a Gould Windograf recorder. The preparation was paced at 2× to 3× diastolic threshold using 2-ms duration stimuli.

Isometric force. The preparation was superfused with a solution containing (mM): NaCl, 135; KCl, 4.5; $MgCl_2$, 2.5, glucose, 5.0; N-(2-hydroxyethyl)piperazine-N′-(2-ethanesulfonic acid), 5.0; Na_2HPO_4, 1.0; aspartic acid, 1.0;

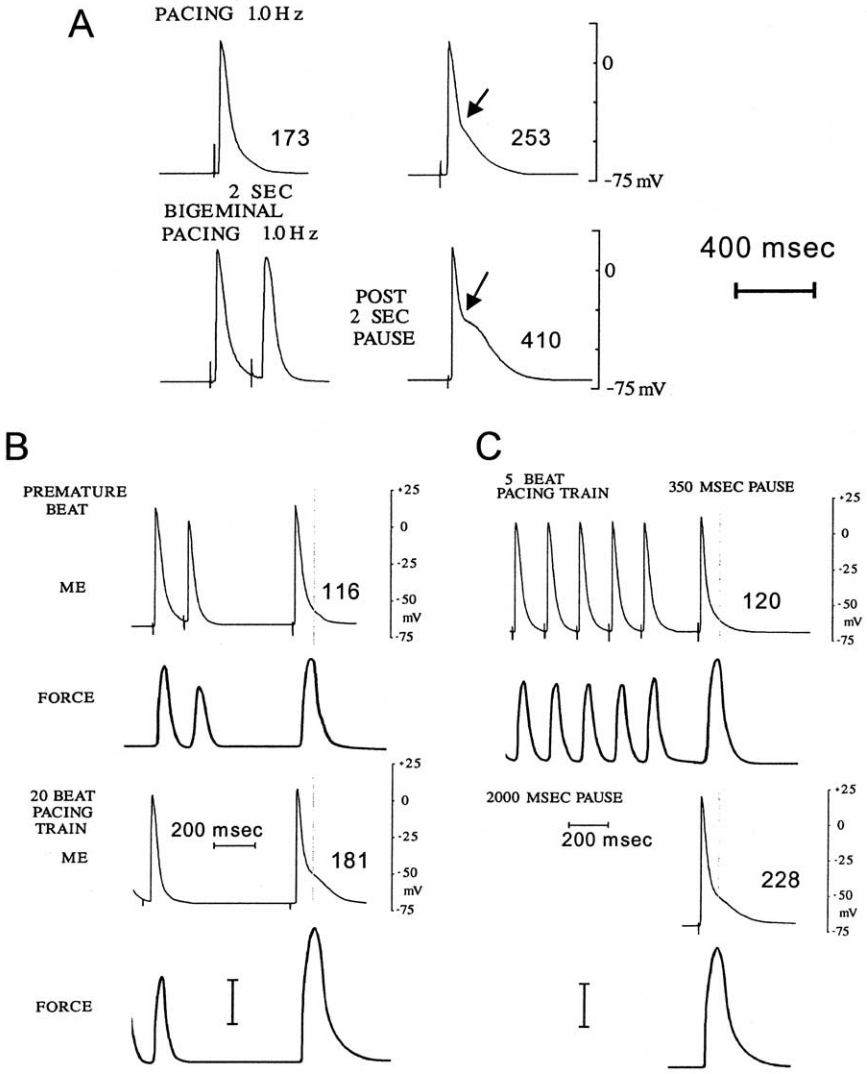

Figure 1. (A) The same action potential is shown during pacing at 1 Hz for 30 s (APD_{90} [an index for the magnitude of early afterdepolarization formation] = 173 ms) followed by a 2-s pause (APD_{90} = 253 ms) and during bigeminal pacing (800:200 ms intervals) for 30 s followed by a 2-s pause (APD_{90} = 410 ms). **(B)** An action potential and isometric force are shown for pacing at 1 Hz interrupted by a premature beat and for a 5-Hz pacing train (20 beats) followed by a 1,000-ms pause. **Vertical lines** mark peak force. **(C)** An action potential and isometric force are shown for pause intervals (350 and 2,000 ms) after a pacing train (5 Hz for five beats). **Vertical calibration bars (B and C)** designate 400 dynes.

JACC Vol. 47, No. 6, 2006
March 21, 2006:1196–206

$CaCl_2$, 2.5, pH adjusted to 7.45 with 5 mM NaOH. The atrial end was mounted in a clamp containing a bipolar pacing electrode, and the distal vein was attached to a Grass FT-01 force transducer. Resting tension was adjusted to achieve maximal isometric force, recorded with a Grass polygraph.

Optical mapping. On removal of the heart from the anesthetized dog (n = 12), the proximal circumflex artery was cannulated and perfused with oxygenated Tyrode solution containing 5 μM 4-(4-ditetradecylaminostyryl)-N-methylpyridinium (ANEPPS) at 35° for 20 min. The anterior descending artery and ventricular branches of the circumflex artery were ligated to enhance atrial perfusion. The preparation was pinned securely to the bottom of the tissue bath, but no drugs or special methods were used to prevent contraction because interventions to limit contraction would alter the Ca^{2+} transient and change the very physiological process that we were studying. The PV sleeve is very thin (<1 mm) and fails to produce vigorous contraction, as shown in the contraction studies, where force generation is very small.

Optical mapping was designed and implemented in accordance with fluorescence characteristics of di-4-ANEPPS, using a charge-coupled device-based digital detector. Comprehensive measurements showed a wide dynamic range (12-bit digitization) and a high temporal resolution (approximately 2 ms). With a 20 × 20-mm field, the system offers spatial resolution of 128 × 128 pixels, 0.156 mm/pixel. With a smaller field, a higher spatial resolution (0.11 mm/pixel) is achieved.

Correctable image distortions or variations are minimized before analysis. These image distortions are usually caused by system components such as vignetting or illumination inhomogeneities. A flat field correction was performed on each of the original digital images. The image pixel values therefore reflect accurately the strength of the fluorescence signal.

Statistics. Data are expressed as the mean ± the standard error. Differences between two groups were determined with the Student test for paired or unpaired determinations, as appropriate. Differences within a group were determined by analysis of variance for repeated measures as appropriate. The Student-Newman-Keuls test was used to determine differences between individual groups when significance was identified by analysis of variance.

RESULTS

Cells within the visible myocardial sleeve, extending 3 to 10 mm from the PV os, had reduced resting potentials (−74 ± 2 mV vs. −79 ± 1 mV, p = 0.008), action potential amplitudes (95 ± 2 mV vs. 102 ± 2 mV, p = 0.009), and APDs at both 50% and 90% of repolarization (58 ± 2 ms and 138 ± 2 ms vs. 76 ± 3 ms and 152 ± 4 ms respectively, p = 0.007 and p = 0.005) compared with adjacent left atrial muscle (n = 76 and 78, respectively) from 43 experimental preparations (left superior PVs, n = 25; right superior PVs, n = 18). Myocardial cells in the vein distal (3 to 5 mm) to the visible sleeve were depolarized (−64 ± 4 mV, p = 0.01), with reduced action potential amplitudes (78 ± 3 mV, p = 0.02) and APDs at both 50% and 90% of repolarization (42 ± 6 ms and 111 ± 7 ms; p = 0.01 and p = 0.005, respectively) (n = 36) compared with PV cells in the visible sleeve. Only microelectrode impalements obtained from the visible PV sleeve are included in the remaining results section.

In the basal state (1.0 Hz), early repolarization is very rapid and the terminal phase of repolarization of the PV sleeve action potential is slowed (Fig. 1A, top left). Interventions amplifying isometric force augmented the delay in repolarization and generated an inflection to a distinctly slowed rate of repolarization that can be characterized as an EAD (Fig. 1A, bottom right). The EAD formation became prominent, and the take-off potential moved to more positive voltages after pacing interventions and catecholamines, interventions shown to increase contractile force.

Table 1. Force Development and EAD Formation With Pacing at 36°C

			Post-Pacing Train Delay (5.0 Hz, 10 Beats)				
	1.0 Hz	Post-PAC	350 ms	500 ms	1,000 ms	2,000 ms	4,000 ms
APD_{90} (ms) (n = 15)	148 ± 4	167 ± 4*	164 ± 3*	190 ± 3*	200 ± 6*	212 ± 5*†	220 ± 5*†
Inflection (mV) (n = 15)	—	−66 ± 6	−64 ± 6	−62 ± 7	−58 ± 7†	−56 ± 6†	−53 ± 7†
Force (dynes) (n = 4)	169 ± 15	398 ± 22*	420 ± 18*	540 ± 16*	642 ± 12*†	720 ± 18*†	754 ± 19*†
Ryanodine − APD_{90} (n = 6)	160 ± 5	161 ± 4	161 ± 5	160 ± 5	161 ± 5	159 ± 5	158 ± 5

		Length of Pacing Train (5.0 Hz, Post-Pacing Pause 1 s)		
	1.0 Hz	5 Beats	10 Beats	20 Beats
Control − APD_{90} (ms) (n = 10)	146 ± 6	184 ± 5*	196 ± 5*‡	216 ± 7*‡
Inflection (mV) (n = 15)	—	−63 ± 6	−58 ± 5‡	−55 ± 8‡
Control − force (dynes) (n = 4)	172 ± 12	346 ± 11*	489 ± 7*‡	523 ± 19*§
Ryanodine − APD_{90} (n = 5)	160 ± 5	159 ± 5	159 ± 5	158 ± 5

*p < 0.02 vs. 1.0 Hz; †p < 0.02 vs. 350 ms; ‡p < 0.05 vs. 5 beats; §p < 0.02 vs. 5 beats.
APD = action potential duration; EAD = early afterdepolarization; PAC = premature atrial contraction.

Pacing interventions. Three pacing algorithms were examined to increase the Ca^{2+} transient: 1) bigeminal pacing, 2) single premature beats, and 3) a prolonged pause after a rapid pacing train. Each intervention increased force generation and enhanced EAD formation. The EAD formation with bigeminal pacing is shown in Figure 1. The APD_{90} (an index for the magnitude of EAD formation because no inflection point may be present under control conditions) observed after a 2-s pause after 30 s of bigeminal pacing increased from 168 ± 12 ms to 312 ± 21 ms ($p = 0.0009$ vs. control) ($n = 15$). Isometric force was more than doubled (168 ± 12 dynes vs. 483 ± 45 dynes, $p = 0.008$) ($n = 5$). Other pacing interventions increasing both APD_{90} and isometric force included: 1) premature beats and 2) rapid pacing trains (Figs. 1B and 1C). Both an increased pause duration after a pacing train and an increased pacing train duration increased isometric force and APD_{90} (Figs. 1B and 1C, Table 1). Although APD_{90} was used to quantitate EAD formation, consistent changes in the EAD inflection point were observed, moving toward depolarization in association with APD_{90} prolongation (Fig. 1, Table 1).

Isometric force and APD prolongation with catecholamines. Norepinephrine and isoproterenol produced concentration-dependent prolongation of APD_{90} (Fig. 2A). At 3.2×10^{-8}M, isometric force was increased four-fold to five-fold with further increases after pacing interventions prolonging APD_{90} (Table 2). Although both catecholamines increased APD_{90}/EAD formation, spontaneous triggering (single beats only) was observed in only 3 of 10 preparations. Single beats (coupling interval = 122 ± 18 ms) arose after pacing-induced pauses (take-off potential = −52 ± 6 mV). Rapid repetitive rhythms were never observed with catecholamines alone. In addition to single beats arising from EADs, there were late-coupled beats arising from delayed afterdepolarizations (DADs) (coupling interval = 225 ± 45 ms) observed in 6 of 10 isoproterenol-

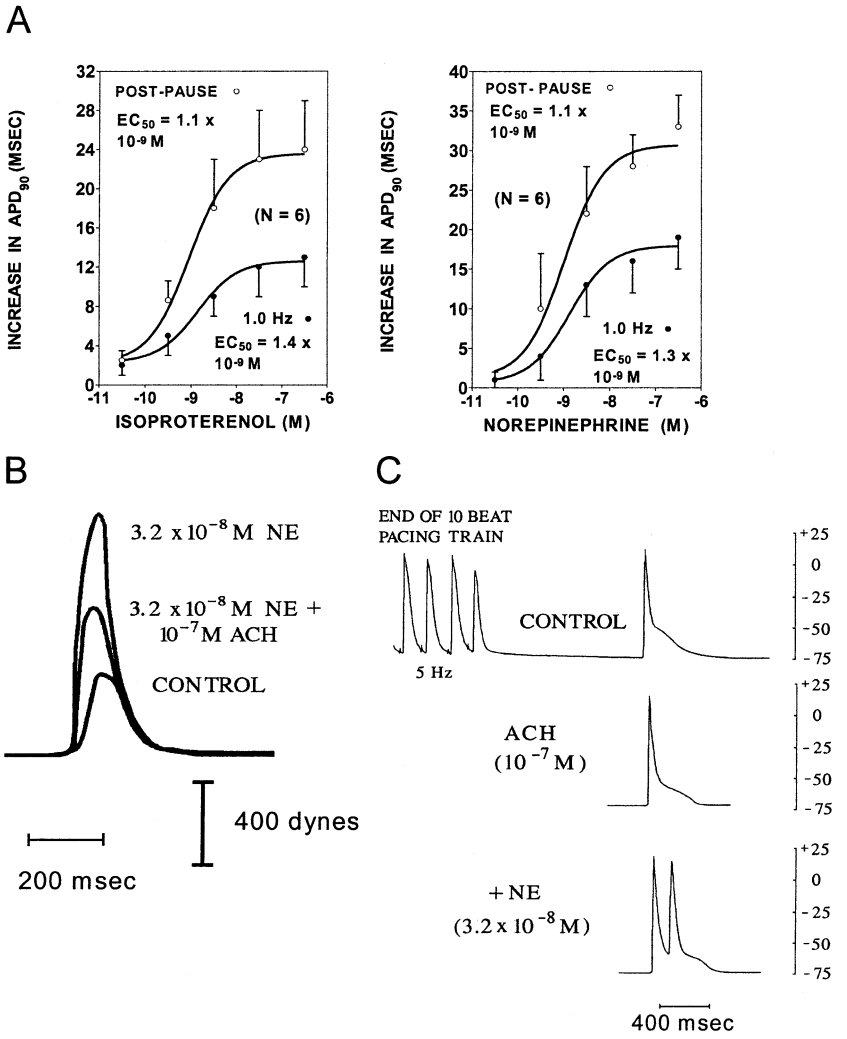

Figure 2. **(A)** Dose-response curves are shown for isoproterenol **(left panel)** and norepinephrine **(right panel)** for APD_{90} [an index for the magnitude of early afterdepolarization (EAD) formation] prolongation (EADs) at 1 Hz **(closed circles)** and for the first beat (post-pause) after a premature beat **(open circles)**. **(B)** Isometric force is shown during 1.0-Hz pacing for control, norepinephrine, and norepinephrine + acetylcholine. **(C)** Action potentials are shown for the first post pacing beat (1.5-s pause) for control, acetylcholine, and acetylcholine + norepinephrine. Addition of norepinephrine resulted in a triggered extrasystole.

Table 2. Force Generation and APD_{90} − Norepinephrine/Isoproterenol + Acetylcholine

	1.0 Hz	Post-PAC	Post-Pacing
Isometric force (dynes) (n = 5)			
Control	176 ± 8	248 ± 11†	544 ± 23
3.2×10^{-8}M norepinephrine	766 ± 43†	832 ± 31†	942 ± 22†
+ 10^{-7}M acetylcholine	429 ± 29†	521 ± 23†	646 ± 24†
3.2×10^{-8}M isoproterenol	802 ± 34†	911 ± 12†	976 ± 39†
+ 10^{-7}M acetylcholine	472 ± 3†	588 ± 15†	698 ± 21†
APD_{90} (ms) (n = 5)			
Control	139 ± 6	168 ± 9	182 ± 11
3.2×10^{-8}M norepinephrine	156 ± 8*	181 ± 10*	202 ± 12*
+ 10^{-7}M acetylcholine	89 ± 10†	102 ± 12†	112 ± 13†
3.2×10^{-8}M isoproterenol	154 ± 6*	166 ± 9*	178 ± 7*
+ 10^{-7}M acetylcholine	78 ± 8†	94 ± 5†	103 ± 6†
APD_{90} (ms) (n = 5)			
Control	139 ± 10	152 ± 9	170 ± 10
3.2×10^{-8}M norepinephrine	151 ± 8*	168 ± 8†	193 ± 12†
+ 10 μM ryanodine	141 ± 8	140 ± 9*	143 ± 10†
3.2×10^{-8}M isoproterenol	149 ± 9*	164 ± 12†	181 ± 10†
+ 10 μM ryanodine	139 ± 9	141 ± 9*	144 ± 2†

*$p < 0.05$ vs. control; †$p < 0.01$ vs. control.
Abbreviations as in Table 1.

treated and 3 of 10 norepinephrine-treated preparations (Fig. 3C).

Role of NCX in EAD formation. Substitution of 30 mM NaCl with 30 mM LiCl (15 min) promoted reverse NCX and Ca^{2+} loading of the sarcoplasmic reticulum, with enhanced EAD formation after a re-introduction of normal Tyrode solution (Na^+ = 130 mM). The take-off potential for EADs was more positive (−57 ± 3 mV to −52 ± 3 mV, $p = 0.035$), and APD_{90} was prolonged. The EAD formation was quickly suppressed by a rapid, transient increase in $[Ca^{2+}]_o$ from 1.35 to 5 mM (n = 5) (Fig. 4A), established by rapid addition of 100 μl 0.73 M calcium chloride during superfusion (20 ml/min).

Diltiazem, in half-log increments every 10 min from 3.2×10^{-9} to 10^{-6}M, failed to alter pause-dependent EAD formation after a premature beat (123 ± 7 ms to 142 ± 7 ms) or a 10-beat pacing train (1-s pause) (199 ± 8 ms) (n = 6). In the presence of 10^{-6}M diltiazem, EAD formation was suppressed by a rapid, transient increase in $[Ca^{2+}]_o$ from 1.35 to 5 mM.

Ryanodine administration. Ryanodine (10 μM for 10 min before re-introduction of normal Tyrode solution) suppressed pause-dependent APD_{90} prolongation associated with premature beats and rapid pacing (Table 1) and catecholamines (Table 2). Examples of suppression of pause-dependent and norepinephrine-induced EAD formation by ryanodine are shown in Figure 4C.

Isometric force and prolongation of APD with hypothermia. Graded hypothermia (32°C to 38°C), increased the duration and magnitude of force development and increased APD (Table 3, Fig. 4B). Further increases in force development, APD, and EAD formation became apparent after pauses produced by a premature beat or after pacing trains. Ryanodine suppressed APD prolongation associated with hypothermia (Table 3).

Combined norepinephrine/isoproterenol + acetylcholine administration. Acetylcholine (10^{-7} M) partially reversed the increase in PV isometric force after isoproterenol or norepinephrine (Table 2, Fig. 2B), but did not eliminate EAD formation (Fig. 2C). After acetylcholine was added, triggered arrhythmias were sustained (Fig. 3A and 3B), lasting >1 s in 26 of 30 preparations and >15 s in 156 of 296 episodes. The longest episode lasted 12 min 33 s. Rapid repetitive rhythms were triggered: 1) by a stimulated beat after a prolonged pause, subsequent to a rapid pacing train (43%), or 2) by a late DAD (cycle length, 218 ± 13 ms) subsequent to rapid non-sustained firing (<1 s) initiated by an early premature stimulus (57%). With reduced acetylcholine concentrations and less APD shortening, triggering was less common (Fig. 3C). Both ryanodine administration and a rapid, transient increase in $[Ca^{2+}]_o$ from 1.35 to 5 mM (n = 6) prevented triggered firing.

The rapid, repetitive firing (59 ± 13 ms cycle length) originated from reduced take-off potentials (−62 ± 6 mV) and showed variable conduction block to other sites, with premature beats capturing multiple recording sites without capturing the site of focal firing (Fig. 3B). Triggered arrhythmia terminated with an EAD (Fig. 3D). The earliest activation site during arrhythmia was always within the proximal as opposed to the distal PV sleeve, as verified by optical mapping (Fig. 5). A concentric pattern of activation indicated a focal rather than a re-entrant mechanism (Fig. 5). We did not detect an excitable gap and double potentials (along a line of block) as previously described for re-entrant arrhythmias arising subsequent to an early premature beat introduced in the presence of acetylcholine alone (12).

DISCUSSION

The EADs associated with prolonged repolarization have been attributed to two mechanisms. Each mechanism is

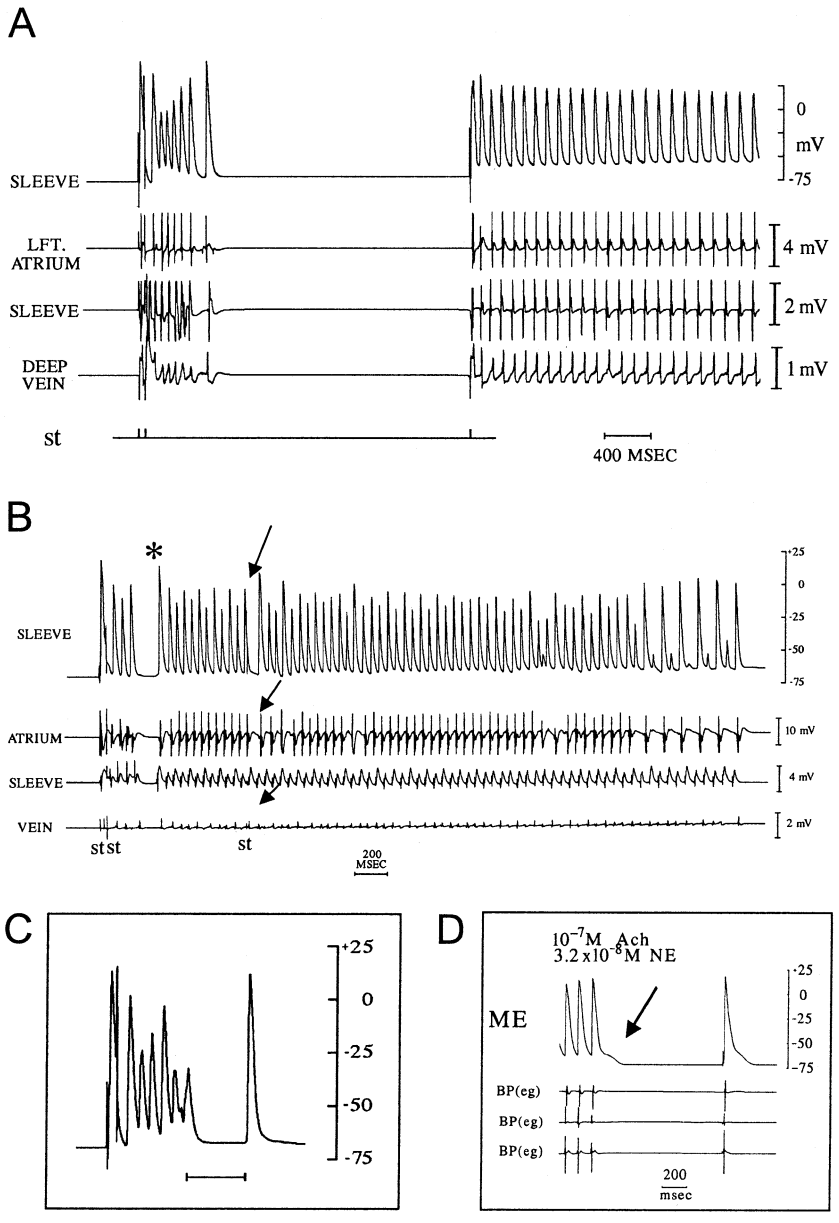

Figure 3. (A) A microelectrode recording from a pulmonary vein (PV) cell shown in conjunction with three electrograms. With norepinephrine (3.2×10^{-8}M) + acetylcholine (10^{-7}M), a premature beat initiates non-sustained firing. After a 4,600-ms pause, the next paced beat initiated sustained firing. **(B)** A PV action potential is shown in conjunction with three electrograms. With norepinephrine (3.2×10^{-8}M) + acetylcholine (10^{-7}M), a single premature beat initiates non-sustained firing. After a 218-ms pause, a spontaneous (non-stimulated) beat **(asterisk)** initiates sustained firing. The timing of the spontaneous beat is similar to that observed at the same norepinephrine concentration, but at a lower acetylcholine (10^{-8}M) concentration **(C)**. Firing is rapid (sleeve) and conducts with variable block to other recording sites. Note that a stimulus (st) applied within atrium captures deep vein, microelectrode, and atrial recording sites **(arrows)** without capturing the arrhythmia focus (sleeve). Termination of a triggered rhythm (18 beats in duration) ending with an early afterdepolarization (EAD) **(arrow)** is shown **(D)**.

critically dependent on delayed repolarization and prolongation of phase 2 of repolarization (plateau). One mechanism implicated in EADs originating at membrane voltages near the plateau ascribes the depolarizing (positive) shift in membrane voltage to reactivation of I_{CaL}, triggering a secondary release of Ca^{2+} from the sarcoplasmic reticulum and secondary contraction (aftercontraction) (9,10). The second mechanism is responsible for EADs generated at membrane voltages negative to I_{CaL} activation, and attributes EADs to Ca^{2+}-activated inward current (I_{NCX}) caused by a secondary "spontaneous" Ca^{2+} release from the sarcoplasmic reticulum (11). With both mechanisms, EADs are intimately associated with aftertransients and aftercontractions. In the present experiments, aftercontractions were not observed in association with EADs that did not generate triggered action potentials; a second contraction was observed only after a non-stimulated/triggered action potential. This finding and the observation of a direct rela-

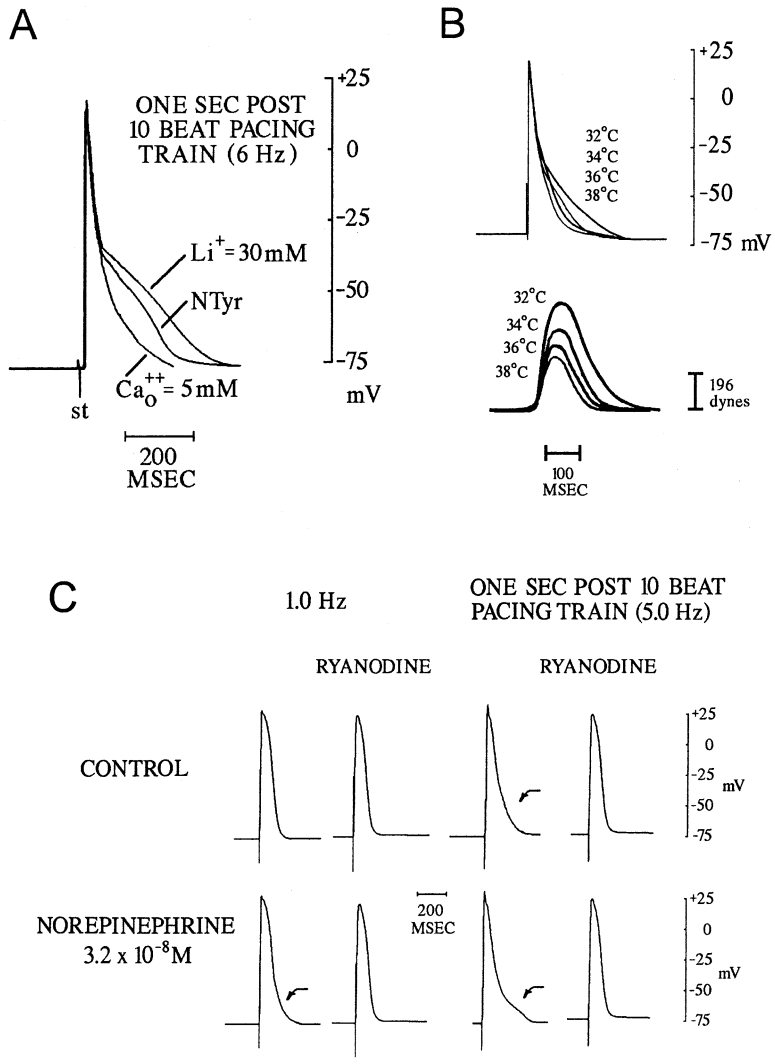

Figure 4. (A) Superimposed action potentials are shown for the first post-pause beat in normal Tyrode solution (NTyr), immediately after the resumption of normal Tyrode solution after superfusion for 15 min with 30 mM LiCl substituting for 30 mM NaCl, and immediately after a transient increase in $[Ca^{2+}]_o$ from 1.35 to 5 mM. **(B)** Superimposed action potentials and force development are shown for 32°C to 38°C. With an increase in isometric force magnitude and duration, terminal repolarization is prolonged. **(C)** Action potentials are shown under control conditions and after norepinephrine, both before and after ryanodine. Recordings are shown both during pacing at 1 Hz **(left panel)** and for the first paced beats observed 1 s after a 10-beat pacing train (5 Hz) **(right panel)**.

tionship between EAD amplitude and triggering versus the amplitude of the contractile force of the primary contraction are the major findings indicating that the mechanism of EAD formation in PV myocytes is directly linked to the primary Ca^{2+} transient. The link to an enhanced primary Ca^{2+} transient distinguishes the present proposed mechanism from mechanisms of EAD formation associated with prolonged APDs. This mechanism is also distinct from delayed afterdepolarizations, which have also been shown to be attributable to a "spontaneous" release of Ca^{2+} under conditions of Ca^{2+} loading (17) and augmented Ca^{2+} sparks (18). The elimination of EADs and triggering by ryanodine and their suppression by transient elevation of $[Ca^{2+}]_o$ support a role for sarcoplasmic reticulum Ca^{2+} release and I_{NCX} (19). The failure of diltiazem to prevent EADs denies a direct role for acute $I_{Ca\text{-}L}$ as a mechanism.

EAD formation in the canine PV: a physiologic event? Inward (forward) I_{NCX} is enhanced by high $[Ca^{2+}]_I$ and negative membrane voltages; conversely, inward I_{NCX} is diminished by high $[Ca^{2+}]_o$. The present experiments show a relationship between isometric force and slow terminal repolarization in PV cells, dependent on inward I_{NCX}. Interventions increasing PV isometric force augment the magnitude and duration of the terminal action potential, taking the form of an EAD (schematic shown in Fig. 6). Conversely, inhibition of sarcoplasmic reticulum Ca^{2+} release by ryanodine attenuated both isometric force and EADs. The data indicate that inward I_{NCX} activated by elevated $[Ca^{2+}]_I$ during the Ca^{2+} transient generates EADs in PVs, enabled by weak repolarizing currents opposing terminal repolarization, including: reduced I_{K1} (7,8), inactivated I_{to}, deactivated I_{Kr}, and activation failure of I_{Ks}.

Table 3. Force Generation and APD_{90} − Hypothermia

n = 5	38°C	36°C	34°C	32°C
Force generation (1.0 Hz)				
1.0 Hz − force (dynes)	169 ± 15	185 ± 15*	239 ± 23†	327 ± 15†
1.0 Hz − force duration (ms)	178 ± 4	193 ± 2*	203 ± 2†	230 ± 4†
1.0 Hz − APD_{90} (ms)	146 ± 4	148 ± 4	158 ± 6*	168 ± 6†
1.0 Hz − APD_{90} (ms) − ryanodine (10 μM)	152 ± 8	154 ± 8	158 ± 7	160 ± 8*
Post-PAC				
Post-PAC − force (dynes)	255 ± 28	289 ± 32*	326 ± 89†	357 ± 32†
Post-PAC − force duration (ms)	183 ± 2	201 ± 5*	203 ± 2†	245 ± 4†
Post-PAC − APD_{90} (ms)	160 ± 6	168 ± 6*	184 ± 9†	200 ± 8†
Post-PAC − APD_{90} (ms) − ryanodine (10 μM)	152 ± 6	154 ± 8	159 ± 8	162 ± 8*
Post 10-beat pacing train (2 s)				
Post-pacing − force (dynes)	375 ± 43	417 ± 41*	434 ± 40*	474 ± 37†
Post-pacing − force duration (ms)	183 ± 2	210 ± 4*	220 ± 5†	250 ± 4†
Post-pacing − APD_{90} (ms)	178 ± 7	187 ± 6*	214 ± 10†	244 ± 11†
Post-pacing − APD_{90} (ms) − ryanodine (10 μM)	156 ± 8	157 ± 9	160 ± 4	162 ± 8*

*$p < 0.05$ vs. 38°C; †$p < 0.01$ vs. 38°C.
Abbreviations as in Table 1.

Contribution of other Ca^{2+}-activated inward currents to EADs, i.e., Ca^{2+}-activated Cl^- current, is not excluded by our experiments. The observations suggest that EADs in PVs are a physiological phenomenon as previously described in rat ventricular trabeculae (20). In both rat ventricle and canine PVs, a slow phase of repolarization (EAD)

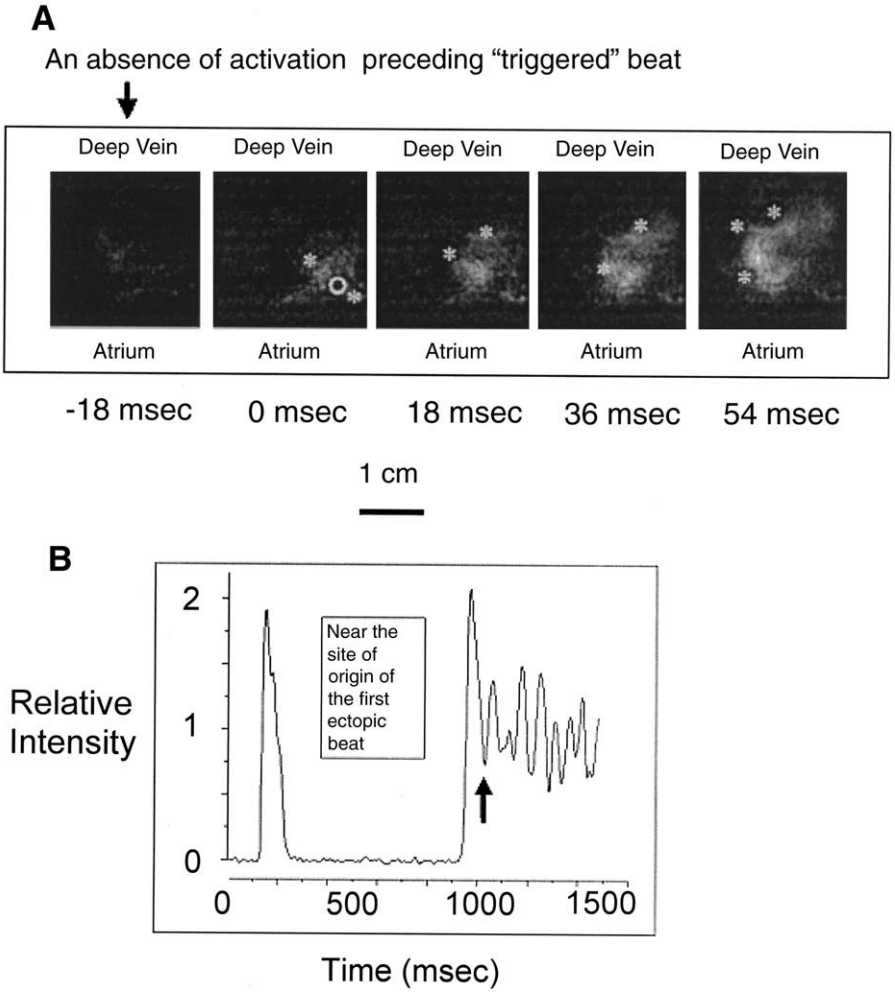

Figure 5. (A) Focal firing is shown in a voltage-activation map during a rapid triggered rhythm during acetylcholine + norepinephrine. The focal firing originates within the pulmonary vein (PV) sleeve. **Asterisks** mark the advancing concentric circular wavefront. The origin marked by the **circle** is shown in **(B)**, voltage recording from the earliest site of activation after a pacing-pause stimulation sequence. **Arrow** = 0 ms.

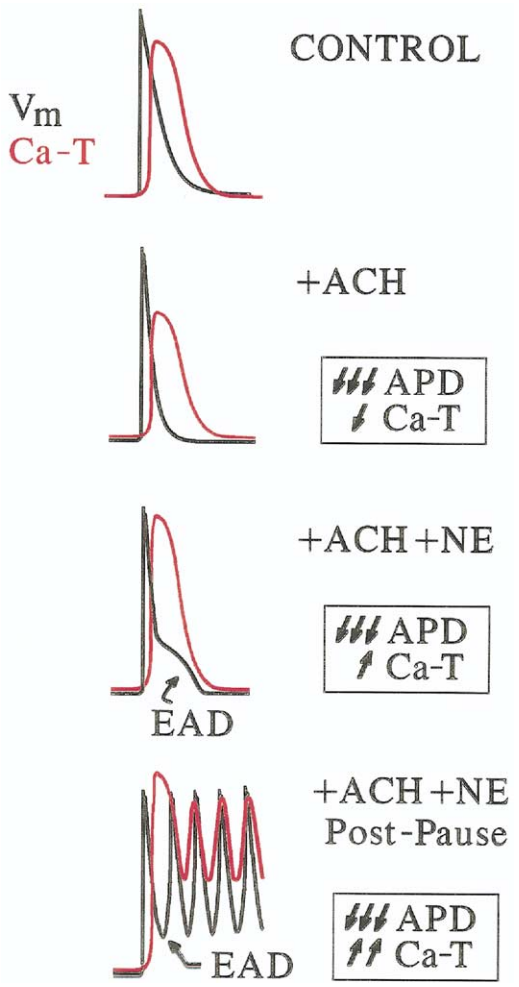

Figure 6. A schematic illustration of the proposed arrhythmia mechanism is shown. Membrane voltage (Vm) is shown in **black**, and the calcium transient (Ca-T) is shown in **orange**. The Ca-T transient outlasts Vm even under control conditions. The difference between the Vm and the Ca-T is increased with action potential duration (APD) shortening observed after acetylcholine (ACH). The early afterdepolarization (EAD) formation is not observed because the Ca-T is also reduced in amplitude. With addition of norepinephrine (NE), the Ca-T is enhanced in amplitude while the APD remains abbreviated. The disparity between Vm and the Ca-T is increased, with inward sodium-calcium exchange (NCX) current producing an EAD. If even further enhancement of the Ca-T is observed after a tachycardia-pause interval, a second action potential is initiated. The Ca-T initiated by the first ectopic beat initiates the second ectopic beat, and so on, producing a repetitive rhythm.

is observed in conjunction with early repolarization and a late inward current synchronous with contraction. In rat ventricle (20) as in the present studies, EADs were suppressed by an increase in $[Ca^{2+}]_o$ and increased with a reintroduction of normal Tyrode solution after exposure to reduced $[Na^+]_o$.

Acetylcholine-induced action potential abbreviation. Although pacing interventions produced dramatic EADs after catecholamines, single triggered extrasystoles were observed infrequently; repetitive firing was never observed. Activation of $I_{K\text{-}Ach}$ by acetylcholine (21) and the resultant decrease in APD (22) was an absolute requirement enabling repetitive triggering in the present studies. With combined catecholamines + acetylcholine, rapid firing could be induced in the PVs by pacing protocols enhancing isometric force and EADs. The inability to capture the focus with premature stimuli, as well as the observation of 2:1 or variable conduction block to other PV sites, is consistent with a rapid, focal rhythm or an extremely small re-entrant circuit.

Muscarinic receptor activation by acetylcholine decreases beta-adrenergic-stimulated cyclic adenosine monophosphate formation (23) and myocardial contractility, limiting the increase in the Ca^{2+} transient by catecholamines and reducing inward I_{NCX} as reflected by the diminution of adrenergic-enhanced EADs by acetylcholine. A further contribution of outward $I_{K\text{-}Ach}$ during late repolarization also would inhibit EAD formation and triggering. Although acetylcholine produces diverse electrophysiologic actions, the net effect was to promote triggering.

Proposed arrhythmogenic mechanism. We propose that the abbreviated APD within PVs determines that peak Ca^{2+} transient occurs during late repolarization. The $[Ca^{2+}]_i$ thus remains elevated at a time when the membrane potential is negative to the equilibrium potential for NCX, activating inward I_{NCX} (Fig. 6). Interventions that further abbreviate repolarization and augment the Ca^{2+} transient enhance EADs and promote triggering. Unlike previously described EAD mechanisms associated with APD prolongation, the present proposed mechanism is critically dependent on accelerated repolarization. Only an enhanced primary Ca^{2+} transient is necessary for triggering, without any need for time-dependent re-activation of I_{CaL} (9,10) or a secondary spontaneous release of Ca^{2+} from the sarcoplasmic reticulum (11). The EADs also may be promoted by a paucity of I_{k1} within PV cells (7,8) and a failure to activate time-dependent I_{Ks}.

A similar mechanism has been proposed for the early AF recurrence in canine atria treated with acetylcholine (24). Increased atrial contractility and triggered beats re-initiating AF were observed with the first beat after AF termination. The investigators attributed late-phase APD prolongation and extrasystoles to rate-induced Ca^{2+} loading with an enhanced Ca^{2+} transient after a prolonged pause. As in the present studies, ryanodine suppresses extrasystole formation.

We used contractile force as a surrogate indicator of relative changes in the Ca^{2+} transient. Although a temporally delayed (and therefore imperfect) indicator of $[Ca^{2+}]_i$, the method estimates the magnitude of the Ca^{2+} transient while avoiding buffering of $[Ca^{2+}]_i$ by a fluorescent indicator. Further experiments using direct determination of the Ca^{2+} transient will be necessary to better understand the coupling of intracellular Ca^{2+} and NCX as an arrhythmia mechanism.

The present experiments conform to the demonstration that stimulation of ganglionated plexuses adjacent to the PVs in intact animals induces PV firing, in turn inducing AF (6). Recently, it was shown in patients with AF that ablation of nerves in the vicinity of the PVs improves successful elimination of AF (25), supporting a facilitory

role for cholinergic and adrenergic input in AF initiated by PV focal firing. Using the same superfused canine PV preparation, local selective autonomic nerve stimulation, with the release of norepinephrine from sympathetic nerve endings and acetylcholine from parasympathetic nerve endings, induced focal firing from the PV sleeve. The triggered firing is dependent on activation of both parasympathetic and sympathetic nerve terminals, as well as an enhanced contractile force development (26). Although the local nerve stimulation may provide a more appropriate physiologic substrate for PV arrhythmia formation, the electrophysiologic bases for EAD formation (sodium-calcium exchange), the dependence of arrhythmia on enhanced rate-dependent EAD formation and contractile force development, and the exclusion of local re-entrant as a primary arrhythmia mechanism (optical mapping) were not performed in the previous published studies, limiting the more precise identification of arrhythmia mechanism allowed in the present studies.

Accelerated early repolarization can also occur in various abnormal conditions including activation of I_{KATP} (ischemia/hypoxia) (27); reduction of I_{Na} (Brugada syndrome) (28); activation of outward currents during early repolarization and inward currents during late repolarization (dilatation and stretch) (29); the short QT syndrome (increased I_k) (30), and reduced I_{CaL} (tachycardia remodeling) (31). The inherent deficiency of I_{K1} in PV myocytes, a facilitory element, could occur when myocytes become depolarized to a membrane voltage at which I_{K1} is reduced by rectification (5,8). The Ca^{2+} loading, also a facilitory element, can occur under both physiological and pathophysiological conditions.

Other mechanisms. The observation of EAD-triggered firing in the present studies does not exclude other mechanisms for PV firing. The EAD-triggered rhythms were often initiated from spontaneous beats observed after a diastolic interval, consistent with a DAD-triggered action potential (Fig. 3B). Although I_f current has been measured in spontaneously firing PV cells, spontaneous firing within intact PV preparations and intact hearts fails to achieve the rapid rates initiating AF in humans, even after catecholamine administration (13).

Honjo et al. (32) have described spontaneous oscillatory beating in rabbit PVs with diastolic depolarization at relatively depolarized membrane voltage initiated by rapid pacing. Ryanodine (0.5 to 2 μM) was used to lock ryanodine channels in the open position to increase $[Ca^{2+}]_i$ with rapid pacing. Experimental manipulations implicated Ca^{2+} release from the sarcoplasmic reticulum, and Ca^{2+} activated I_{NCX} and I_{Cl} in the generation of the oscillatory activity occurring at rates less rapid than observed in present experiments. The present experiments used a larger ryanodine concentration (10 μM) that completely suppressed sarcoplasmic reticulum Ca^{2+} release, preventing the development of the Ca^{2+} transient and associated NCX current.

The fertile potential of the extremely short action potential within PVs to support re-entry has been well recognized and shown by us in the superfused canine PV preparation exposed to acetylcholine (but not adrenergic agonists) (12). It is possible that re-entry is a mechanism to sustain tachyarrhythmias initiated by triggering in this preparation exposed to both acetylcholine and adrenergic agonists, although not elucidated by our experiments using optical mapping. The optical mapping provided convincing data to support a focal mechanism of EAD triggering for the initiation of the rhythm disturbances, and this is supported by the presence of a long diastolic interval preceding the beat that initiated the first ectopic beat. A long diastolic interval allowing a complete recovery of refractoriness within the PV is highly unfavorable for the initiation of re-entry. Certain changes during the sustained tachycardia would oppose the operation of sustained triggering, including the intracellular accumulation of sodium, to reverse Na-Ca exchange with enhancement of K^+ currents. We also favor sustained triggering as a mechanism in the present experiments because the rhythms are faster (1,132 $\pm$ 53 beats/min) than re-entrant arrhythmias documented by optical mapping (832 $\pm$ 82 beats/min). Both short (3- to 6-beat duration) and prolonged (more than 15 s in duration) rapid rhythms initiated by rapid pacing followed by a pause frequently terminate with an EAD, as shown in Figure 3D. We cannot, however, exclude a role for re-entry.

Reprint requests and correspondence: Dr. Eugene Patterson, 6E103 ET CARI, 1200 Everett Drive, Oklahoma City, Oklahoma 73104. E-mail: eugene-patterson@ouhsc.edu.

REFERENCES

1. Haissaguerre M, Jais P, Shah DC, et al. Spontaneous initiation of atrial fibrillation by ectopic beats originating in the pulmonary veins. N Engl J Med 1998;339:659–66.
2. Hsieh MH, Chen SA, Tai CT, et al. Double multielectrode mapping catheters facilitate radiofrequency catheter ablation of focal atrial fibrillation originating from pulmonary veins. J Cardiovasc Electrophysiol 1999;10:136–44.
3. Jais P, Meleze H, Laurent M, et al. Distinctive electrophysiological properties of pulmonary veins in patients with atrial fibrillation. Circulation 2002;106:2479–85.
4. Cheung DW. Electrical activity of the pulmonary vein and its interaction with the right atrium in the guinea pig. J Physiol 1980; 314:445–56.
5. Chen Y, Chen S, Chang M, Lin C. Arrhythmogenic activity of cardiac muscle in pulmonary veins of the dog: implication for the genesis of atrial fibrillation. Cardiovasc Res 2000;48:265–73.
6. Schauerte P, Scherlag BJ, Patterson E, et al. Focal atrial fibrillation: experimental evidence for a pathophysiologic role of the autonomic nervous system. J Cardiovasc Electrophysiol 2001;12:592–9.
7. Chen Y-J, Chen S, Chen Y-C, et al. Effects of rapid atrial pacing on the arrhythmogenic activity of single cardiomyocytes from pulmonary veins: implication in initiation of atrial fibrillation. Circulation 2001; 104:2849–54.
8. Ehrlich JR, Tae-Joon C, Zhang L, et al. Cellular electrophysiology of canine pulmonary vein cardiomyocytes: action potential and ionic current properties. J Physiol 2003;551:801–13.
9. January CT, Riddle JM. Early afterdepolarizations: mechanism of induction and block: a role for L-type Ca^{2+} current. Circ Res 1989; 64:977–90.
10. Luo CH, Rudy Y. A dynamic model of the cardiac ventricular action potential. II. Afterdepolarizations, triggered activity, and potentiation. Circ Res 1994;74:1097–113.

11. Szabo B, Sweidan R, Rajagopalan CV, Lazzara R. Role of Na^+:Ca^{2+} exchange current in C_S^+-induced early afterdepolarizations in Purkinje fibers. J Cardiovasc Electrophysiol 1994;5:933–44.
12. Po SS, Li Y, Tang D, et al. Rapid and stable reentry within the pulmonary vein as a mechanism initiating paroxysmal atrial fibrillation. J Am Coll Cardiol 2005;45:1871–7.
13. Arora R, Verheule S, Luis S, et al. Arrhythmogenic substrate of the pulmonary veins assessed by high-resolution optical mapping. Circulation 2003;107:1816–21.
14. Kalifa J, Jalife J, Zaitsev AV, et al. Intra-atrial pressure increases rate and organization of waves emanating from the superior pulmonary veins during atrial fibrillation. Circulation 2003;108:665–71.
15. Hocini M, Ho S, Kawara T, et al. Electrical conduction in canine pulmonary veins: electrophysiological and anatomic correlation. Circulation 2002;105:2442–8.
16. Krishnan SC, Antzelevitch C. Flecainide-induced arrhythmia in canine ventricular epicardium. Phase 2 reentry? Circulation 1993;87:562–72.
17. Wier G, Hess P. Excitation-contraction coupling in cardiac Purkinje fibers. Effects of cardiotonic steroids on the intracellular [Ca^{2+}] transient, membrane potential, and contraction. J Gen Physiol 1984;83:395–415.
18. Nishio M, Ruch SW, Kelly JE, et al. Ouabain increases sarcoplasmic reticulum calcium release in cardiac myocytes. J Pharmacol Exp Ther 2004;308:1181–90.
19. Bers DM, Bridge JHB, MacLeod KT. The mechanism of ryanodine action in cardiac muscle assessed with Ca selective microelectrodes and rapid cooling contractures. Can J Physiol Pharmacol 1987;65:610–8.
20. Schouten VJ, ter Keurs HE. The slow repolarization of the action potential in rat heart. J Physiol 1985;360:13–25.
21. Shi H, Yang B, Xu D, Wang H, Wang Z. Electrophysiologic characterization of cardiac muscarinic acetylcholine receptor; different subtypes mediate different potassium currents. Cell Physiol Biochem 2003;13:59–74.
22. Webb JW, Hollander PB. The action of acetylcholine and epinephrine on the cellular membrane potentials and contractility of rat atrium. Circ Res 1956;4:332–6.
23. Watanabe AM, Lindemann JP, Fleming JW. Mechanisms of muscarinic modulation of protein phosphorylation in intact ventricles. Fed Proc 1984;43:2618–23.
24. Burashnikov A, Antzelevitch C. Reinduction of atrial fibrillation immediately after termination of the arrhythmia is mediated by late phase 3 early afterdepolarization-induced triggered activity. Circulation 2003;107:2355–60.
25. Pappone C, Santinelli V, Francesco M, et al. Pulmonary vein denervation enhances long-term benefit after circumferential ablation for paroxysmal atrial fibrillation. Circulation 2004;109:327–34.
26. Patterson E, Po SS, Scherlag BJ, Lazzara R. Triggered firing in pulmonary veins initiated by in vitro autonomic nerve stimulation. Heart Rhythm 2005:2:624–31.
27. Noma A. Existence of K channels sensitive to intracellular ATP in cardiac cells as revealed by a modified inside-out patch recording technique. Biomed Res 1986;7:95–8.
28. Brugada P, Brugada J. Right bundle branch block, persistent ST-segment elevation and sudden cardiac death; a distinct clinical and electrocardiographic syndrome, a multicenter study. J Am Coll Cardiol 1992;20:1391–6.
29. Bode F, Sachs F, Franz M. Biochemistry: tarantula peptide inhibits atrial fibrillation. Nature 2001;409:35–6.
30. Brugada R, Hong K, Dumaine R, et al. Sudden death associated with short-QT syndrome linked to mutations in HERG. Circulation 2004;109:30–5.
31. Yue L, Feng J, Gaspo R, et al. Ionic remodeling underlying action potential changes in a canine model of atrial fibrillation. Circ Res 1997;81:512–25.
32. Honjo H, Boyett MR, Niwa R, et al. Pacing-induced spontaneous activity in myocardial sleeves of pulmonary veins after treatment with ryanodine. Circulation 2003;107:1937–43.